Environmental Earth Sciences (2020) 79:314
https://doi.org/10.1007/s12665-020-09059-3

ORIGINAL ARTICLE

Geoelectrical characterisation of CO_2–water systems in porous media: application to carbon sequestration

K. O. Rabiu[1,2] · R. Van der Helm[1] · N. Mumford[1] · D. B. Das[1]

Received: 14 August 2017 / Accepted: 15 June 2020 / Published online: 23 June 2020

Abstract

Carbon sequestration is a promising method for the reduction of carbon dioxide (CO_2) emissions as it permits the storage of compressed CO_2 in the subsurface. The carbon sequestration sites must be monitored to detect potential leaks; one possible method involves the monitoring of geoelectrical properties such as electrical conductivity (σ_b) and dielectric constant (ε_b). This investigation focuses on using a time domain reflectometry (TDR) sensor to determine the influence of different factors on the measurements of the electrical conductivity (σ_b) and dielectric constant (ε_b) of a porous rock reservoir in relation to the soil water saturation (S_w). The factors investigated were presence of surfactant, salt concentration, pH and rock type which are unique to a given storage site. A number of dynamic two-phase flow experiments were performed using gaseous CO_2. It was found that salt concentration, rock type and presence of a surfactant had a notable effect on the σ_b–S_w and ε_b–S_w relationships. Higher salt concentrations were found to give higher values for σ_b and ε_b for given S_w values. Limestone was found to result in the highest values of both σ_b and ε_b for any given S_w, followed by silica and basalt samples. The presence of a surfactant resulted in higher values for σ_b at higher S_w values and lower values for σ_b at lower S_w values compared to the case when no surfactant was present. Surfactant presence also resulted in lower values for ε_b at given S_w values. Initial pH values (with silica sand) were found to have no significant effect on the σ_b–S_w and ε_b–S_w relationships. The measurements of σ_b and ε_b indicate that the use of TDR presents a viable monitoring option. Furthermore, statistical analysis using non-linear regression was carried out on the experimental results and the model shows a good reliability in the prediction of the monitoring process in geological carbon sequestration.

Keywords Time domain reflectometry · Water saturation · Carbon sequestration · Geoelectrical monitoring · Salt concentration · pH · Anionic surfactant

Introduction

Global warming due to anthropogenic greenhouse gas production is widely regarded as one of the major issues threatening the planet (Solomon et al. 2009). One method for reducing excessive atmospheric CO_2 emission is carbon capture and sequestration (CCS); a general term for the capture, transport and storage of carbon dioxide from the atmosphere or large emission sources. An effective form of sequestration is geological sequestration, whereby carbon dioxide in gaseous, liquid, supercritical or dissolved form is injected underground into porous rock formations typically at depths larger than 1 km for long-term storage (Ansolabehere et al. 2007). The supercritical conditions of CO_2 exist above temperatures of 31.1 °C and pressure of 73.9 bar. Under these conditions, CO_2 exhibits properties of both liquid phase and gaseous phase. For example, CO_2 will occupy a container like a gas but with liquid density (Petrik and Mabee 2011; Metz et al. 2005).

Notably, suitable formations for CO_2 storage include deep saline aquifers, basalts, hydrocarbon reservoirs and unmineable coal seams located at a depth of 800 m or above, where pressures and temperatures of the reservoirs keep the CO_2 in liquid or supercritical condition (Franceschina et al. 2015; Metz et al. 2005). If all the sedimentary basins worldwide are considered for CCS, the storage capacity for CO_2 in geological formations would be enormous; however, the

✉ D. B. Das
D.B.Das@lboro.ac.uk

[1] Chemical Engineering Department, Loughborough University, Loughborough, LE LE11 3TU, UK

[2] Present Address: Civil Engineering Department, Osun State University, Osogbo, Nigeria

acceptability of any specific storage site depends on many features such as proximity to CO_2 sources, possibility for leakages and other specific factors such as permeability and porosity (Folger 2009).

It is important to know that for CCS to become a successful climate change mitigation option, it must be possible to securely store CO_2 underground for millennia without leakage into the atmosphere; and to ensure that the CO_2 is successfully trapped, the reservoir sites must be monitored (Khudaida and Das 2014; Benson and Cole 2008). Geological CO_2 storage can occur through four main trapping mechanisms: physical barriers, capillary forces, solubility trapping, and mineralisation (Ansolabehere et al. 2007; Abidoye et al. 2015; Khudaida and Das 2014). Although carbon sequestration is an economically and ecologically viable method, the carbon must be effectively trapped to avoid leakages back into the atmosphere or undesirable migration to shallow aquifers via fractures, permeable pathways and nearby penetrable wells, whereby potable water could become contaminated (Abidoye and Das 2015b).

Monitoring techniques can also minimize the risks of CO_2 leakage, because it gives early warning of CO_2 storage problem, in other words, it quantifies the amount of CO_2 storage (Hartai 2012). Many geophysical techniques exist to monitor carbon sequestration (Kiessling et al. 2010; Hovorka et al. 2011).

Geoelectrical characterization of the carbon sequestration presents a simple and non-invasive monitoring method as it can relate the electrical properties of the rock formation to its water saturation (White et al. 2003; Abidoye et al. 2015), which is directly related to the CO_2 content of the reservoir. Two main electrical properties exist: the electrical conductivity, σ_b (a metric for the current induced upon application of an electric field or ability of an aqueous solution to carry electric current) and the dielectric constant, ε_b (a metric for the electrical polarization induced upon application of an electric field) (Keller 1966; Han 2011). These are suitable parameters for monitoring because of their sensitivity to changes in saturation of the water-CO_2 phase (Abidoye and Das 2015a). A time domain reflectometry (TDR) sensor, which is inexpensive and presents a reliable and simple technique to measure both σ_b and ε_b, is a potential sensor for the measurement of these parameters as it can be incorporated underground around the area of storage.

It is observed in the literature that seismic method also provides an effective monitoring technique to assess CO_2 plume. A repeated seismic survey is important for ensuring both containment and conformance monitoring. Seismic method has been shown to be an excellent monitoring method to quantify small amount of CO_2 saturations in the reservoir, but it has been less successful in determining the increase in CO_2 saturation (Furrea et al. 2017; Alfia et al. 2019). Electromagnetic and electric methods are also important tools for monitoring CO_2. They utilise the electrical and electromagnetic responses from the subsurface to determine the changes in CO_2 or water saturations. The methods involve the quantification of electric parameters such as resistivity and conductivity and, determining the correlations such as the Archie expression to relate these parameters to saturations. Methods that use these concepts are the electrical resistivity tomography (ERT), electromagnetic resistivity (ER), electromagnetic induction tomography (EMIT) among others (Ajayi et al. 2019). Dafflon et al. (2012) explained the importance of electrical resistance tomography (ERT) in monitoring the migration of groundwater with dissolved CO_2. As the electrical response of rocks is highly independent of the mechanical response, electrical and seismic quantifications provide complementary estimates of CO_2 saturation (Daley 2019).

To date, most CO_2 sequestration projects involve injecting CO_2 in supercritical phase (Metz et al. 2005; Hosa et al. 2010; Abidoye and Das 2015a). Although the storage of CO_2 in supercritical form can be safer and more effective, it is important to consider the high cost of compression from gaseous to supercritical phase (Petrik and Mabee, 2011). In addition, the implication of injecting $ScCO_2$ under high pressure during the injection process can cause natural disasters such as earthquakes (Bachu 2000; Metz et al. 2005). Therefore, this work focused on using both the gaseous and supercritical CO_2. Research has shown that gaseous CO_2 has been used as an alternative to supercritical CO_2 (see, e.g., U.S Department of Energy 2008). Nonetheless, commercial scale of CO_2 storage in gaseous form is very unlikely because of its unfavourable risk assessment. This study is also important, because CO_2 stored in supercritical condition may leak due to faulty caprock and form a gaseous phase. Therefore, if monitoring sensors are situated at lower depth of the reservoir (i.e., 200–400 m), the sensor can detect the gaseous CO_2 when there is leakage. A wide range of geoelectrical monitoring methods have been developed to monitor the movement and storage of injected supercritical CO_2 (Rabiu et al. 2017; Abidoye and Das 2015a), yet there is an outstanding need to find out whether this robust tool can track gaseous CO_2 efficiently and effectively.

Characteristics of some of the geological rock formations currently used for carbon sequestration have been

Table 1 Typical characteristics of deep saline aquifers used for carbon sequestration (Ranganathan et al. 2011; Rempel et al. 2011; De Silva et al. 2015; Metz et al. 2005)

Parameter	Values
Porosity	0.18–0.30
Depth (km)	0.6–2.7
T (°C)	35–98
P (bar)	70–285
Salt conc. w/w %	5–20
pH	5.4–8.1

summarised in Table 1. The rock types being investigated are silica, limestone and basalt; with silica and limestone being the most ubiquitous rock types in deep saline aquifers (Bentham and Kirby 2005; De Silva et al. 2015). Basalt is also investigated as it offers the possibility of improving carbon mineralisation and thus provides permanent CO_2 storage (Matter and Kelemen 2009; Adam et al. 2011; Rabiu et al. 2017). Therefore, to effectively relate the geoelectrical characteristics to the water saturation, the factors influencing these electrical properties must be properly understood. Previous studies have shown that σ_b and ε_b are influenced by temperature, pressure, rock type, salt concentration, surfactants, permeability, mineralogy and clay content (Rabiu et al. 2017; Abidoye and Das 2015a, b; Han 2011; Magill 2009; Carcione et al. 2012) when injecting liquid or supercritical CO_2 into a bed of sand particles. The purpose of this study is to understand how these factors affect the measurements, for which there is currently little data and significant uncertainty as to the extent to which these factors affect these parameters.

The work of Rabiu et al. (2017) characterised CO_2 sequestration in silicate, limestone and basalt using geoelectrical properties. But their investigation was limited on liquid and $ScCO_2$ phases. Earlier, the works of Kaszuba et al. (2003) as well as Abidoye and Das (2015a) investigated supercritical CO_2 trapping in porous materials. Therefore, it can be concluded that most of the existing publications focus on injecting liquid and supercritical CO_2 in porous media. However, the important question concerning whether gaseous CO_2 and $scCO_2$ have the same effect on geoelectrical properties remains unanswered. This work explores this gap in knowledge by investigating geoelectrical characterisation of CO_2 sequestration during the injection of gaseous CO_2.

Experimental

Solutions

All artificial brine solutions were created with analytical grade sodium chloride (NaCl) salt acquired from Fisher Scientific (Loughborough, UK) and distilled water. For the experiments using surfactant, the brine solution was created using 0.2 g of Plantacare 1200 UP (BASF SE, Ludwigshafen, Germany) to create a 0.02% w/w surfactant solution. Before each experiment, the pH of the saturated sand sample was measured with a pH meter (Fisher Scientific, Loughborough). The first pH measurement of silica sand after saturated with brine water is 6.1 ± 0.2. For the experiments at pH 8.1, the pH of the saturated sand sample was adjusted to pH 8.1 ± 0.2 using 0.02 M NaOH.

Porous media

For the success of any CO_2 sequestration project, the porous materials must be fully characterised to know whether the reservoir is suitable for the storage. In this work, three porous rock types were tested: silica sand (Minerals Marketing Company, Cheshire, UK), limestone (Tarmac Buxton Lime and Cement, Buxton, UK), and basalt sand (Aqua Maniac, Delaware, USA). The characteristics of porous sample such as porosity and average particle size were determined experimentally and are listed in Table 2. The properties of the silica, basalt and limestone sand were designed to be almost the same but could not be precisely be the same. For example, all the three materials were sieved manually with six sieves of sizes ranging from 762 to 1557 µm to obtain similar average particle size. The porosity of the material was determined by packing sand into a cylinder of known volume and saturating the bed with a measured amount of water. The porosity was then calculated using Eq. 1:

$$\emptyset = \frac{V_t - V_s}{V_t} = \frac{V_v}{V_t} = \frac{V_w}{V_t}, \quad (1)$$

where $\emptyset$ is porosity, V_t is the total volume of a porous media sample, V_s is the volume of solids in the sample, V_v is the volume of openings (voids), and V_w is the volume of water that will occupy the voids space. Before use, the sands were rinsed with distilled water and dried to eliminate any clay content.

Experimental rig

A CO_2 flow rig (Fig. 1) was designed and constructed in this work. The rig was composed of a bespoke 4 cm high sample holder (i.d. 10 cm) situated in a PID-controlled heating cabinet (West Control Solutions, Brighton, UK) connected to a CO_2 syringe pump and controller (Teledyne ISCO Incorporated, Nebraska, USA). The stainless-steel sample holder, composed of a cell and end-pieces at the top and bottom, contained an inlet for CO_2 at the top, and an outlet for water at the bottom, lined with a hydrophobic and

Table 2 Characteristics of the sand samples used in the experiments

Parameters	Silica sand	Limestone sand	Basalt sand
Porosity (%)	39 ± 0.25	40 ± 0.30	42 ± 0.30
Average particle size (µm)	968 ± 253	1147 ± 270	1016 ± 296

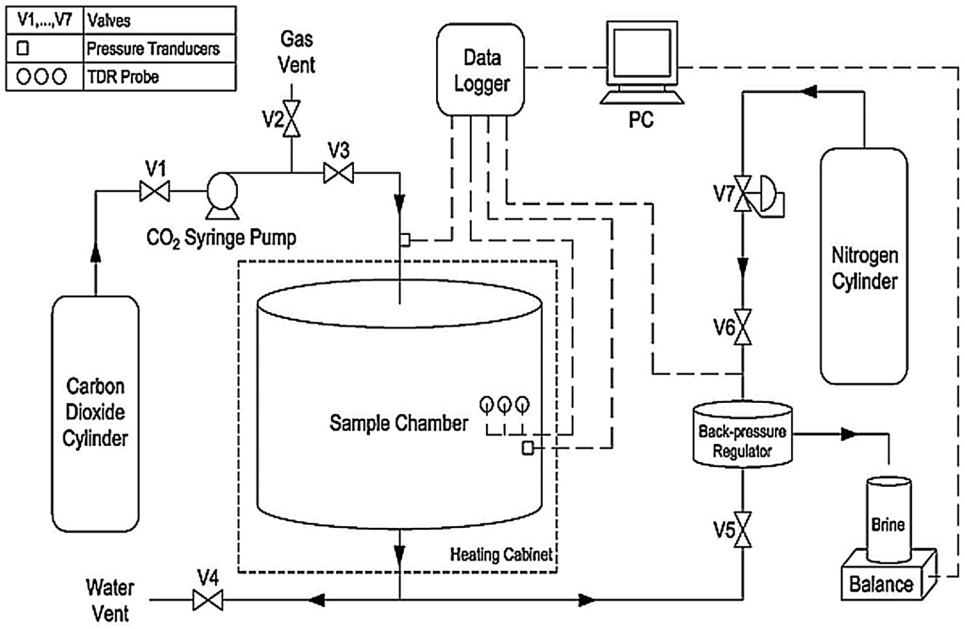

Fig. 1 Schematic diagram of the experimental setup (adapted from Rabiu et al. 2017)

hydrophilic membrane, respectively, to prevent water from exiting the top and CO_2 from exiting the bottom (Porvair Filtration Group Ltd, Hampshire, UK). Figure 1 shows a schematic diagram of the experimental setup with the TDR probe (Campbell Scientific Limited, Shepshed, UK) at the centre of the sample holder. Measurements from the probe and the transducers were transmitted to the computer via a datalogger.

Experimental procedure

Before each experiment, a small amount of the relevant brine solution was added to the sample chamber followed by 500 g of the relevant rock particles. The remaining brine was added until the sample was completely saturated and trapped air was removed by gentle pressing. The mass to volume ratio for each of the sand particles sample were ensured to be the same (i.e., 500 g of sand particles sample was used for each experiment). The chamber was sealed via the addition of the lid and tightening of bolts. The CO_2 syringe pump was filled with gaseous carbon dioxide at 55 bar and 23 °C from the pressurized cylinder (BOC gases, Leicester, UK). The temperature was set to 23 °C, and carbon dioxide was released into the chamber via the syringe pump at a flow of 2 mL/min.

The flow rate of exiting brine was mediated to give a low brine flow rate by adjusting the Nitrogen gas back-pressure from a pressurized cylinder (BOC gases, Leicester, UK) using valve V5. Once brine ceased to flow out from the chamber, the experiment was terminated. Before dismantling of the rig, the CO_2 was vented from the chamber through V2. Thereafter, the rock particles were evacuated, washed and recycled for use in further experiments. In addition, the chamber was rinsed with tap water to ensure that all sand particles were removed before subsequent experiments.

Results and discussion

Repeatability of experiments

Figure 2a, shows the reproducibility of results for σ_b and ε_b, respectively. As mentioned in previous study (Abidoye and Das 2015a), σ_b has been found in several studies (Huang et al. 2005; Plug et al. 2007; Keller 1966) to be a function of water saturation. It is inferred that σ_b increases with greater presence of water, because liquid water is a superior conductor of electricity than gaseous carbon dioxide.

Since permittivity (ε_b) of water is greater than the gaseous CO_2 and silica sand (Drnevich et al. 2001), it is this to which the trend shown in Fig. 2b can be attributed to. At high values of water saturation, ε_b is high, in accordance with the high dielectric constant value for water. As the CO_2 concentration within the sample holder increases, due to its high resistance (Breen et al. 2012), the dielectric constant decreases towards that of the silica sand. At the lowest value of water saturation, the dielectric constant approaches the value of 2.5–3.5 for silica sand (Drnevich et al. 2001). Results for dielectric constant show a comparable trend to that obtained by Plug et al. (2007). The maximum percentage difference is 50% but, in their work, they used distilled water; the present work utilised the brine water which is commonly found in the saline

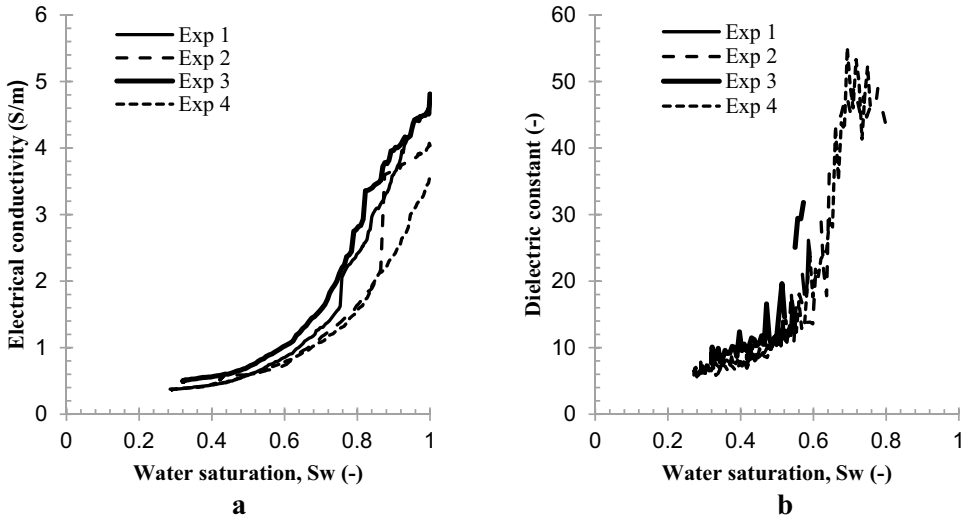

Fig. 2 **a** σ_b–$S_{w,}$ **b** ε_b–S_w curves for four repeated experiments at a salt concentration of 5% w/w NaCl (55 bar, pH 6.1, silica sand)

aquifers. However, the maximum percentage of 3% was obtained for the experiment using distilled water (see, e.g., Rabiu et al. 2017).

Effect of salt concentration

As can be seen from Fig. 3a, b, salt concentration has a significant effect on both σ_b and ε_b. At a given $S_{w,}$ the σ_b is greater for higher salt concentrations, since σ_b is a function of the concentration of ions present (Singha et al. 2012; Coury 1999). The difference between the conductivities at greater S_w becomes more pronounced.

At a given S_w, ε_b is greater for higher salt concentrations. This is attributed to the presence of more ions; therefore, greater polarization induced when an electric field is applied. As can be noted from Fig. 3b, significant fluctuations are present within the ε_b–S_w curves. There is more fluctuation in ε_b at higher salt concentration making it impossible to find the values of ε_b as the S_w approaches 1 for the 2% and 5% solutions. This can be explained by the large concentration of ions (and thus their increased mobility) interfering with the TDR dielectric constant measurements. Hu et al. (2011) discovered that this effect can be mitigated by coating the TDR probe with an insulating layer. There is little difference between the results for 0.5% and 2% salt concentration, especially at lower S_w. However, there is a sizeable difference between 5 and 2% salt concentrations, suggesting that the relationship between pH and ε_b is not linear. Sea water has an average salinity of approximately 3.5% (http://hyperphysics.phy-astr.gsu.edu/hbase/chemical/seawater.html), which is comparable to the concentrations used in the experiment. The values of approximately 5.3 S/m (Bullard, 1995) and 70–80 (Fores, 1999) for σ and ε of seawater, respectively,

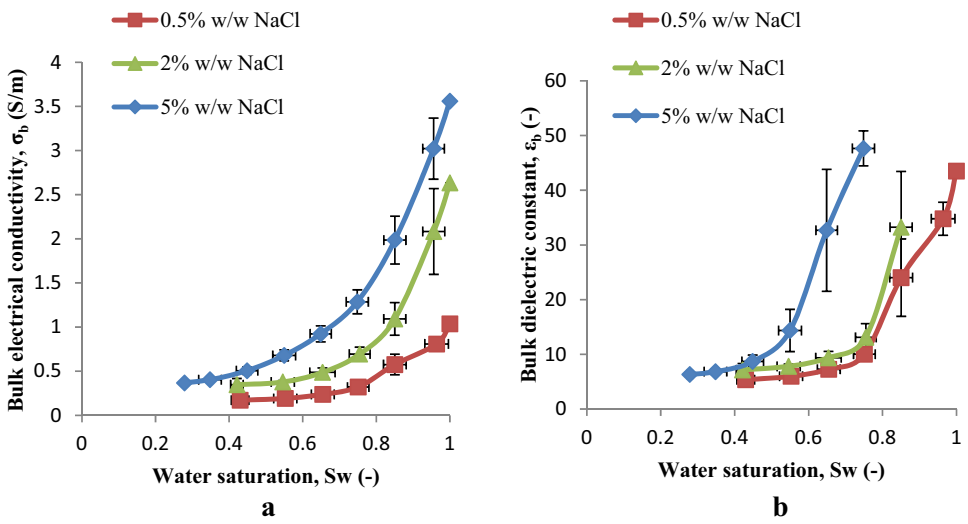

Fig. 3 **a** σ_b–S_w and **b** ε_b–S_w curves at salt concentrations 0.5, 2, 5% w/w NaCl (55 bar, 23 °C, silica sand, pH 6.1)

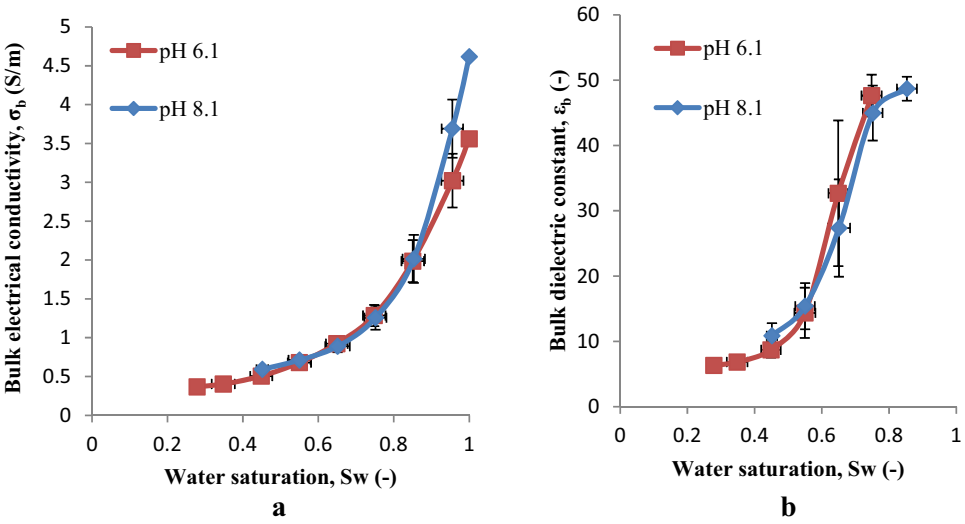

Fig. 4 **a** σ_b–S_w and **b** ε_b–S_w curves for brine solutions at pH 6.1 and 8.1 (55 bar, 23 °C, 5% w/w NaCl, silica sand)

are in the same order of magnitude as the values obtained at maximum S_w.

As can be seen from Fig. 4a, b showing the effect of pH on the σ_b–S_w and ε_b–S_w curves, a change in the initial pH of the brine solution has no significant impact. Although σ_b at $S_w = 1$ at pH 8.1 is slightly higher than σ_b at pH 6.1 (3.5 ± 0.5 S/m vs 4.6 ± 0.4 S/m), this difference is due to the increased ion concentration due to the higher pH. For both the σ_b and ε_b, a significant difference in results was expected by changing the pH of the solution.

Effect of pH

It has been reported that alkaline pH favours the reactions in mineralisation (Druckenmiller and Mercedes Maroto-Valer 2005: Matter et al. 2007), hence reducing the ion concentration within the sample holder. As no changes in σ_b were recorded, it can be assumed that no mineralisation reactions occurred. This is due to the fact that the ions typically required for CO_2 mineralisation (i.e., Ca^{++}, Mg^{++}, Fe^{++}, K^{+}) are not present within the solution (De Silva et al. 2015). In addition, the absence of mineralisation can also be attributed to the limited duration of the experiment, since mineralisation occurs over a longer period.

Effect of rock type

As can be seen from Fig. 5a, b, the rock type present in the sand body has a significant effect on both the σ_b and ε_b curves. While σ_b in Fig. 5a is relatively similar for silica and basalt, sizeable differences are noticed in the limestone. At $S_w = 1$ the average σ_b for limestone (4.9 ± 0.8 S/m) is significantly higher than for silica or basalt sand (3.7 ± 0.5 S/m and 3.6 ± 0.6 S/m, respectively). This trend is observed throughout the S_w range (at 30% water saturation, the limestone

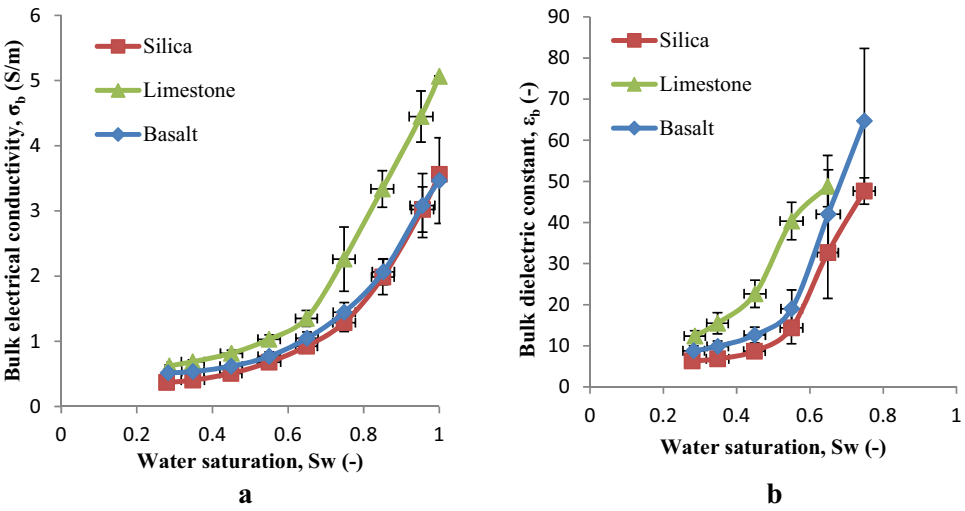

Fig. 5 **a** σ_b–S_w and **b** ε_b–S_w curves for silica, limestone and basalt sand experiments (55 bar, 23 °C, 5% w/w NaCl)

curve is above the silica and basalt curves). This effect can be explained by the fact that σ_b for limestone is higher than that of silica (Duba, et al. 1978) and basalt sands (Hyndman and Drury 2007). Abidoye and Das (2015b) attribute the heightened σ_b of the limestone to the dissolution of limestone in water and thereby increased concentration of dissolved ions (Plan 2005; Assayag, et al. 2009). Figure 5b shows the relationship between ε_b and S_w for the different rock types. As with the σ_b curve, ε_b for limestone is consistently higher than that for silica and basalt. This was also observed by Abidoye and Das (2015b). This is consistent with the bulk ε_b values for the rocks (Dutta and De 2007; Martinez and Byrnes 2001; Rust et al. 1999; ElShafie and Heggy 2012). The difference in dielectric properties can be attributed to their chemical constituents (Abidoye and Das 2015a).

Nelson and Trabelsi (2012) state that the factors which influence the permittivity of the material include density, porosity, pore structure, material composition and signal frequency. However, since the porosity measurements of the materials were very similar (see Table 2), it can be argued that these do not affect ε_b.

Effect of temperature

Storing CO_2 in supercritical condition is generally acceptable because of its favourable properties (i.e., water related density and gaseous viscosity) which can make it to store significant amount of CO_2 (Metz et al. 2005; Petrik and Mabee 2011). Besides, it is safer to store CO_2 in supercritical phase, because it minimises the effect of leakage during buoyancy (Khudaida and Das 2014; Metz et al. 2005). However, a perturbation in the temperature of the reservoir can change the CO_2 phase completely, either into gaseous or liquid phase and this can have an effect on geoelectrical properties during the monitoring process. This work investigated the temperature effect on the σ_b–S and ε_b–S relationship and the results are displayed in Fig. 6a, b, respectively. It is observed that the σ_b and ε_b rise as the temperature increases in silica sand system. Similarly, the work on the effect of temperature on geoelectrical properties and water saturation relationship has been carried out on silica, basalt and limestone sand by injecting liquid and supercritical CO_2 (Rabiu et al. 2017; Abedian and Baker 2008; Or and Wraith 1999; Abidoye and Das 2015a). Gaseous CO_2 was injected in the current work, because it is assumed that a change in the CO_2 phase might have an effect on the geoelectrical properties. The results in Fig. 6a show an increasing trend in temperature as the electrical conductivity (σ_b). A similar trend was noticed in the work of Rabiu et al. (2017) and Abidoye and Das (2015a) but in their work, liquid and supercritical CO_2 phases were used. This can be attributed to the increase in the mobility of ions at high temperature. In addition, an increase in temperature results in an increase in dielectric permittivity (ε_b), and this can be related to the bound water released during the experiment (Abidoye and Das 2015a).

Effect of surfactant

In addition to being used in enhanced oil recovery, surfactants are also used in carbon sequestration to improve displacement efficiency and aqueous solubility of carbon (Magill 2009). As can be seen from Fig. 7a comparing the σ_b-S_w curves for systems with and without surfactant, the presence of surfactant has a substantial effect on σ_b. At $S_w = 1$, σ_b with surfactant is higher than with no surfactant (6 ± 0.4 S/m vs 3.8 ± 0.4 S/m), likely due to the presence of additional ions in the solution. However, at $S_w < 0.75$,

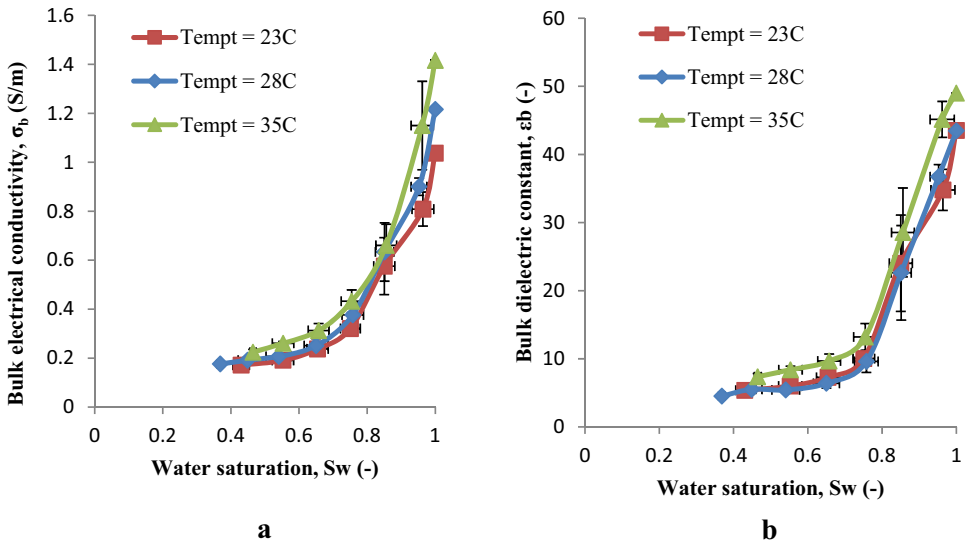

Fig. 6 **a** σ_b–S_w, **b** ε_b–S_w curves at temperature 23 °C, 28 °C, 35 °C (55 bar, silica sand, 0.5% w/w NaCl)

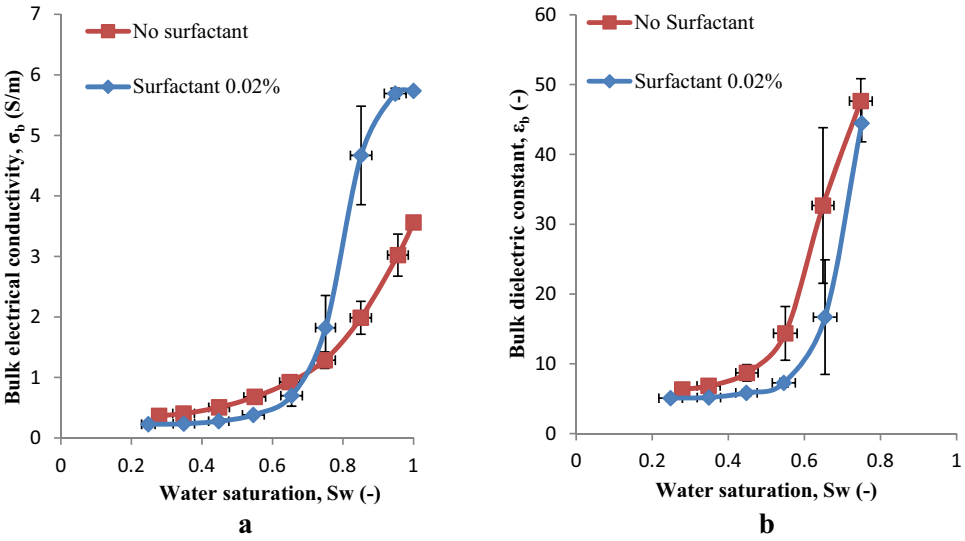

Fig. 7 **a** σ_b–S_w, **b** ε_b–S_w curves for systems with and without surfactant (5% w/w NaCl, 55 bar, 23 °C, gaseous CO_2)

σ_b with surfactant is lower than without surfactant. It could be hypothesized that it is related to the reduced mobility of the ions caused by presence of large surfactant molecules increasing the viscosity of the brine solution (Jewell et al. 2015; Wu et al. 2014).

The ε_b–S_w curve with surfactant shown in Fig. 7b is consistently below the ε_b–S_w without surfactant. This can be explained by the increased viscosity of the surfactant solution. This would increase resistance to the molecules lining up in response to the application of an electric field, resulting in reduced polarity. The experiments with higher concentration of surfactant have some limitations, for example, there is excessive foam which affects the accuracy of σ_b–S_w and ε_b–S_w relationships.

Comparison between gaseous CO_2 and $ScCO_2$

Carbon capture and sequestration is a viable technology to avert the problem of CO_2 emission from fossil fuel. However, more knowledge is required to fully understand the behaviour of the subsurface during geological storage of carbondioxide. Ideally, CO_2 is stored in supercritical phase due to its favourable properties (i.e., higher density and viscosity). A significant amount of CO_2 is stored in this form in comparison to the injection of gaseous CO_2. On the other hand, the compression of gaseous CO_2 into supercritical CO_2 is very expensive. Besides, the high pressure of the supercritical CO_2 injection can affect the earth surface and consequently cause earthquakes (Bachu 2000; Metz et al. 2005). While the majority of CO_2 sequestration and monitoring processes have been carried out in supercritical condition

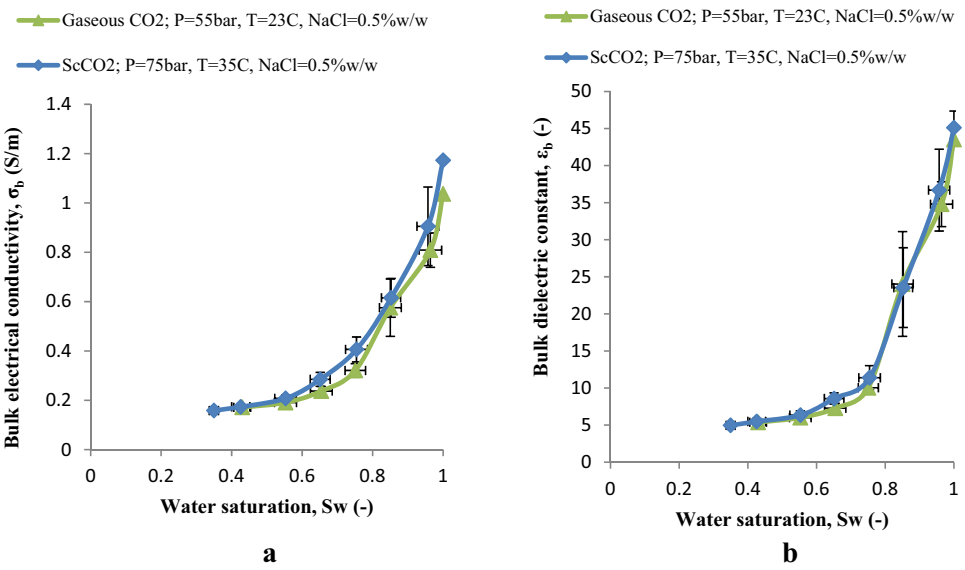

Fig. 8 **a** σ_b–S_w and **b** ε_b–S_w curves for silica sand systems with gaseous and $ScCO_2$

(Rabiu et al. 2017; Abidoye and Das 2015a, b; Metz et al. 2005), there is a possibility of monitoring the gaseous CO_2 in the subsurface. Recently, Lamert et al. (2012) explored the monitoring of gaseous CO_2. In their work, gaseous CO_2 was injected into the subsurface for monitoring purposes. Figure 8a, b shows the σ_b–S_w and ε_b–S_w curves for systems with gaseous and $ScCO_2$. The σ_b–S_w curve is higher in supercritical condition than in gaseous form. This effect can be attributed to the phase change and higher temperature in the supercritical phase. However, the ε_b–S_w curve shows no significant difference between $ScCO_2$ and gaseous CO_2, although a slight increase is observed in supercritical phase when compared with gaseous phase. In the future work, high pressure and temperature will be used for $ScCO_2$ which will provide significantly different experimental conditions allowing analysis in a much broader range of conditions.

Regression of experimental data

The dielectric permittivity (ε) of air, sand particles and water are 1, 3 and 80, respectively. The differences in these values cause the bulk dielectric permittivity to be related to water saturation (Abidoye and Das 2015a; Rabiu et al. 2017). The experimental results from this study were fitted to Archie's law (Archie, 1942). The equation is written as follows:

$$\sigma_b = \frac{s^n}{\emptyset^{-m}}\sigma_w, \tag{2}$$

where S is the water saturation, $\emptyset$ is the sand porosity, σ_b = bulk conductivity, σ_w is the brine conductivity, n is the saturation exponential and m is the cementation exponential.

From the above Eq. (2), exponent m and n can be deduced using non-linear regression statistical analysis. The analysis was used to fit the value of m and n for each of the porous materials studied (silica, basalt and limestone). The logarithm linearization of Eq. (2) is shown in Eqs. (3) and (4):

$$\log \sigma_b - m \log \emptyset = \log \sigma_w + n \log S \tag{3}$$

$$n \log S + m \log \emptyset = \log \sigma_b - \log \sigma_w. \tag{4}$$

The values of the exponents m and n for silica, basalt and limestone using Minitab statistical analysis are shown in Table 3.

The m and n values from the non-linear regression using the Minitab statistical software (Microsoft 2016) are in agreement with previous studies (see, e.g., Scudiero et al. 2012; Wang et al. 2014; Abidoye and Das 2015a; Rabiu et al. 2017; Liu and Moysey 2012). It can be deduced that Achie's equation can be used to predict the experimental results.

Table 3 Exponents m and n values for silica, basalt and limestone (Archie 1942)

Porous media	m (–)	n (–)
Silica	1.701	1.768
Basalt	1.260	1.559
Limestone	1.296	1.132

Moreover, the statistical software was used to predict the value of dielectric permittivity (ε_b). The value of ε_b is paramount, because it characterizes the degree of water saturation in the sand system. The bulk dielectric permittivity, ε_b is, therefore, can be written as

$$\varepsilon_b = f(S, P, T, i), \tag{5}$$

where S is the water saturation, P is the pressure, T is the temperature, and i is the initial value of ε_b before CO_2 injection.

The non-linear regression polynomial model equation is generated from experimental results using Minitab statistical software. The equation is shown in Eq. (6):

$$\begin{aligned}\varepsilon_b = & -699.547 + 86.470S + 55.992T \\ & + 1.743P - 13.475i - 8.103S^2 \\ & - 1.015T^2 - 0.024P^2 + 0.244i^2.\end{aligned} \tag{6}$$

The regression results in using Eq. (6) are shown in Fig. 9a, b. The figures reveal that the model provides a good match for the experimental data, because most of the data are fitted accurately (coefficient of correlation (R^2) in Figs. 9a, b are 0.8570 and 0.8295, respectively). In particular Eq. (6) shows that ε_b (and hence, CO_2 saturation) can be estimated based on four common measurable quantities of the geological formation, namely, saturation, temperature, water pressure and initial ε_b. Simple approximation of the process such as in Eq. (6) can help take managerial decisions faster and accurately. They also offer cost benefits over other complex methods of gathering the required information on the real process. It is, therefore, envisaged this model can be used to predict the behaviour of CO_2 in subsurface during CO_2 sequestration.

Conclusions

The effect of different factors on σ_b–S_w and ε_b–S_w relationships in porous rock media were investigated using a TDR probe. Salt concentration, rock type and presence of surfactant had an observable effect on the relationships; however, different initial values of pH (with silica sand) produced no significant change. Higher salt concentrations were shown to result in higher σ_b and ε_b values for a given S_w, which was attributed to the greater number of ions present. For any given S_w, limestone was found to give higher values of both σ_b and ε_b, followed by basalt and silica, respectively. For σ_b, this can be explained by a greater level of

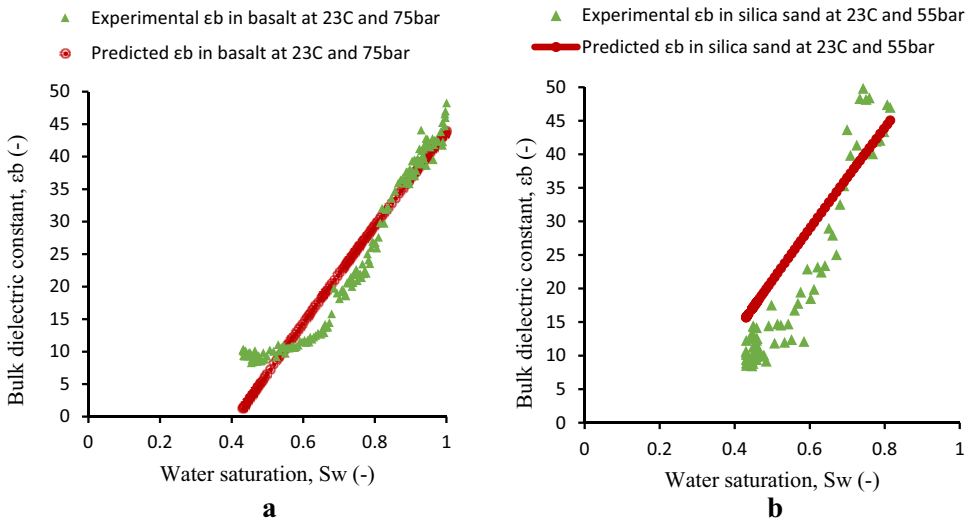

Fig. 9 Model of permittivity values in **a** CO_2–brine–basalt sand ($R^2 = 0.86$) and **b** CO_2–brine–silica sand ($R^2 = 0.83$) systems using non-linear regression

dissociation of the rock, resulting in a greater number of ions in solution.

In the case of ε_b, the difference can be attributed to their respective chemical compositions. Presence of surfactant resulted in lower σ_b values at lower S_w values and higher σ_b values at higher S_w values compared with solution absent of surfactant. ε_b values were found to be lower in the presence of surfactant at any given S_w. These differences can be attributed to the increase in viscosity due to the surfactant. Although change in initial pH was found to produce no discernible change in the relationships with silica sand, it was hypothesized that an effect could be observed with a different rock type.

This work contributes to the understanding of the effect of salt concentration, pH, rock type and surfactant presence on σ_b–S_w and ε_b–S_w relationships. Measuring σ_b and ε_b is a viable option for monitoring CO_2 storage sites, and consequently understanding how these geoeletrical parameters relate to S_w is essential. This enables an estimate to be made from the measured geoelectrical parameters, which in turn relates to the CO_2 content of the storage site. Therefore, by monitoring the geoelectrical characteristics, changes in CO_2 content indicative of leakage can be detected. The Archie equation was used to predict the experimental results and the outputs were corroborated with previous studies. Finally, a fit regression analysis was carried out on the experimental results and the model reveals a good reliability in the prediction of monitoring process in geological carbon sequestration.

Acknowledgements The authors are grateful to Tertiary Education Trust Fund (TETFund), Nigeria for a Ph.D. scholarship to Kazeem Rabiu which made this work possible. Comments of three anonymous referees are also acknowledged which helped to improve the quality of this paper.

References

Abedian B, Baker KN (2008) Temperature effects on the electrical conductivity of dielectric liquids. IEEE Trans Dielectr Electr Insul 15:888–892. https://doi.org/10.1109/TDEI.2008.4543127

Abidoye LK, Das DB (2015a) Geoelectrical characterization of carbonate and silicate porous media in the presence of supercritical CO_2-water flow. Geophys J Int 203:79–91

Abidoye LK, Das DB (2015b) pH, geoelectrical and membrane flux parameters for the monitoring of water-saturated silicate and carbonate porous media contaminated by CO_2. Chem Eng J 262:1208–1217

Abidoye LK, Das DB, Khudaida KJ (2015) Geological carbon sequestration in the context of two-phase flow in porous media: a review. Crit Rev Environ Sci Technol 45:1105–1147

Adam L, Otheim T, Wijk K, Batzle M, McLing T, Podgorney R (2011) CO_2 sequestration in basalt: carbonate mineralization and fluid substitution. SEG Technical Program Expanded Abstracts: 2108–2113. https://doi.org/10.1190/1.3627626

Ajayi T, Gomes JS, Bera A (2019) A review of CO_2 storage in geological formations emphasizing modeling, monitoring and capacity estimation approaches. Pet Sci. https://doi.org/10.1007/s12182-019-0340-8

Alfia M, Vascob DW, Hosseinic SA, Meckelc TA, Hovorka SD (2019) Validating compositional fluid flow simulations using 4D seismic interpretation 1 and vice versa in the SECARB early test—a critical review. Int J Greenh Gas Control 82:162–174. https://doi.org/10.1016/j.ijggc.2019.01.003

Ansolabehere S, Beer J, Deutch J, Ellerman D, Friedmann J, Herzog H, Jacoby H, Joskow P, Mcrae G, Lester R, Moniz E, Steinfeld E, Katzer J (2007) The future of coal: options for a carbon constrained world. Massachusetts Institute of Technology, Cambridge. https://web.mit.edu/coal/The_Future_of_Coal.pdf. Accessed 15 Nov 2019

Archie GE (1942) The electrical resistivity log as an aid in determining some reservoir characteristics. Trans Am Inst Min Metall Eng 146:54–61

Assayag N, Matter J, Ader M, Goldberg D, Agrinier P (2009) Water–rock interactionsduring a CO_2 injection field-test: implications on host rock dissolution and alteration effects. Chem Geol 265:227–235

Bachu S (2000) Sequestration of CO_2 in geological media: criteria and approach for site selection in response to climate change. Energy Convers Manag 41:953–970

Benson SM, Cole DR (2008) CO_2 sequestration in deep sedimentary formations. Elements 4:325–331

Bentham M, Kirby G (2005) CO_2 storage in saline aquifers. Oil Gas Sci Technol 60(3):559–567

Breen SJ, Carrigan CR, LaBrecque DJ, Detwiler RL (2012) Bench-scale experiments to evaluate electrical resistivity tomography as a monitoring tool for geologic CO_2 sequestration. Int J Greenh Gas Control 9:484–494

Bullard E (1995) 2.7.9 Physical properties of sea water. In: Kaye & laby-table of physical & chemical constants. National Physical Laboratory, New Delhi

Carcione JM, Gei D, Picotti S, Michelini A (2012) Cross-hole electromagnetic and seismic modeling for CO_2 detection and monitoring in a saline aquifer. J Petrol Sci Eng 100:162–172

Coury L (1999) Conductance measurements part 1: theory. Curr Sep 18(3):91–96

Dafflon B, Wu Y, Hubbard SS, Birkholzer JT, Daley TM, Pugh JD, Peterson JE, Trautz RC (2012) Monitoring CO_2 intrusion and associated geochemical transformations in a shallow groundwater system using complex electrical methods. Environ Sci Technol 47(1):314–321

Daley TM (2019) Rock physics of CO_2 storage monitoring in porous media. Geophys Geosequestration. https://doi.org/10.1017/9781316480724.005

De Silva G, Ranjith P, Perera M (2015) Geochemical aspects of CO_2 sequestration in deep saline aquifers: a review. Fuel 155:128–143

Drnevich VP, Yu X, Lovell J, Tishmack J (2001) Temperature effects on dielectric constant determined by time domain reflectometry. School of Civil Engineering, Purdue University, West Lafayette

Druckenmiller M, Mercedes Maroto-Valer M (2005) Carbon sequestration using brine of adjusted pH to form mineral carbonates. Fuel Process Technol 86:1599–1614

Duba A, Piwinskii A, Santor M, Weed H (1978) The electrical conductivity of sandstone, limestone and granite. Geophys J R Astron Soc 53:583–597

Dutta K, De S (2007) Electrical conductivity and dielectric properties of SiO_2 nanoparticles dispersed in conducting polymer matrix. J Nanopart Res 9:631–638

ElShafie A, Heggy E (2012) Dielectric properties of volcanic material and their role for assessing rock hardness in the maritian subsurface. In: 43rd Lunar and planetary science conference, held March 19–23, 2012 at The Woodlands, Texas. https://www.lpi.usra.edu/meetings/lpsc2012/pdf/2790.pdf. Accessed 15 Feb 2020

Folger P (2009) Carbon capture and sequestration (CCS). Congressional research service reports. http://digitalcommons.unl.edu/cgi/viewcontent.cgi?article=1043&context=crsdocs. Accessed 10 July 2017

Fores GR (1999) The dielectric properties of sea water. [Online] http://www.ieec.cat/hosted/oppscat/KNMI_slides/node21.html. Accessed 4 June 2017

Franceschina G, Augliera P, Lovati S, Massa M (2015) Surface seismic monitoring of a natural gas storage reservoir in the Po Plain (northern Italy). Bollettino di Geofisica Teorica ed Applicata 56(4):489–504. https://doi.org/10.4430/bgta0165

Furrea A, Eiken O, Alnes H, Vevatne JN, Kaer AF (2017) 20 years of monitoring CO_2-injection at Sleipner. In: 13th international conference on greenhouse gas control technologies, GHGT-13, 14–18 November 2016, Lausanne, Switzerland, Energy procedia, vol 114, pp 3916–3926. https://doi.org/10.1016/j.egypro.2017.03.1523

Han X (2011) Determination of soil critical water content with bulk soil electrical conductivity. (M.Sc. Thesis), Florida State University, USA. http://purl.flvc.org/fsu/fd/FSU_migr_etd-4295. Accessed 12 Jan 2017

Hartai E (2012) Carbon dioxide storage in geological reservoirs. Institute of Mineralogy and Geology. http://fold1.ftt.uni-miskolc.hu/~foldshe/co2geol.pdf. Accessed 25 Oct 2017

Hosa A, Esential M, Stewart J, Haszeldine S (2010) Benchmarking worldwide CO_2 saline aquifer injections. Scottish Centre for Carbon Capture and Storage: 1–67. https://era.ed.ac.uk/bitstream/handle/1842/15681/wp-2010-03-1.pdf?sequence=2. Accessed 10 Dec 2019

Hovorka SD, Meckel TA, Trevino RH, Lu J, Nicot J, Choi J, Freeman D, Cook P, Daley TM, AjoFranklin JB, Freifeild BM, Doughty C, Carrigan CR, Brecque D, Kharaka YK, Thordsen JJ, Phelps TJ, Yang C, Romanak KD, Zhang T, Holt RM, Lindler JS, Butsch RJ (2011) Monitoring a larger volume CO_2 injection: year two results from SECARB project at Denbury's Cranfield, Mississippi, USA. Energy Procedia 4:3478–3485

Hu G, Ye Y, Diao S, Zhang J, Liu C (2011) Time domain reflectometry (TDR) in measuring water contents and hydrate saturations in marine sediments. In: Proceedings of the 7th international conference on gas hydrates (ICGH 2011), Edinburgh, Scotland, UK, July 17-21, 2011. http://www.pet.hw.ac.uk/icgh7/papers/icgh2011Final00156.pdf. Accessed 3 July 2017

Huang X, Xu Y, Karato S (2005) Water content in the transition zone from electrical conductivity of wadsleyite and ringwoodite. Nature 434(7034):746–749

Hyndman R, Drury M (2007) Physical properties of basalts, gabbros, and ultramafic rocks. In: Deep sea drilling project initial reports, vol 37. Deep Sea Drilling Database, pp 395–401

Jewell S, Zhou X, Apple ME, Dobeck LM, Spangler LH, Cunningham AB (2015) Bulk electric conductivity response to soil and rock CO_2 concentration during controlled CO_2 release experiments: observations and analytic modeling. Geophysics 80(6):E293–E308. https://doi.org/10.1190/geo2014-0118.1

Kaszuba JP, Janecky DR, Snow MG (2003) Carbon dioxide reaction processes in a model brine aquifer at 200 °C and 200 bars: implications for geologic sequestration of carbon. Appl Geochem 18:1065–1080. https://doi.org/10.1016/S0883-2927(02)00239-1

Keller GV (1966) Electrical properties of rocks and minerals. Geol Soc Am Mem 97:553–577

Khudaida KJ, Das DB (2014) A numerical study of capillary pressure-saturation relationship for supercritical carbon dioxide (CO_2) injection in deep saline aquifer. Chem Eng Res Des 92:3017–3030

Kiessling D, Hattenberger C, Hartmut S, Schilling F, Krueger K, Schoebel B, Danckwardt E, Kummerow J (2010) Geoelectrical methods for monitoring geological CO_2 storage: First results from the cross-hole and surface-downhole measurements from the CO2SINK test site at Ketzin (Germany). Int J Greenh Gas Control 4:816–826

Lamert H, Geistlinger H, Werban U, Schutze C, Peter A, Hornbruch G, Schulz A, Pohlert M, Kalia S, Beyer M, Grobmann J, Dahmke A, Dietrich P (2012) Feasibility of geoelectrical monitoring and multiphase modeling for process understanding of gaseous CO_2 injection into a shallow aquifer. Environ Earth Sci 67(2):447–462

Liu Z, Moysey SM (2012) The dependence of electrical resistivity-saturation relationships on multiphase flow instability. ISRN Geophys 212:1–11. https://doi.org/10.5402/2012/270750

Magill MT (2009) Geoelectrical response of surfactant solutions in a quartzitics and analog aquifer. UNLV Theses/Dissertations/Professional Papers/Capstones, Las Vegas

Martinez A, Byrnes A (2001) Modeling dielectric-constant values of geologic materials: an aid to ground-penetrating radar data collection and interpretation. Curr Res Earth Sci 241:1–16

Matter JM, Kelemen PB (2009) Permanent storage of carbon dioxide in geological reservoirs by mineral carbonation. Nat Geosci 2(12):837–841. https://doi.org/10.1038/ngeo683

Matter JM, Takahashi T, Goldberg D (2007) Experimental evaluation of in situ CO_2-water-rock reactions during CO_2 injection in basaltic rocks: Implications for geological CO_2 sequestration. Geochem Geophys Geosyst 8(2):1–19

Metz B, Davidson O, Coninck H, Loos M, Meyer L (2005) IPCC special report on carbon dioxide capture and storage, Intergovernmental Panel on Climate Change, Geneva (Switzerland). Working Group III. Cambridge University Press. https://www.ipcc.ch/pdf/special-reports/srccs/srccs_wholereport.pdf. Accessed 28 Sep 2019

Nelson OS, Trabelsi S (2012) Factors influencing the dielectric properties of agricultural and food products. J Microw Power Electromagn Energy 46(2):93–107

Or D, Wraith JM (1999) Temperature effects on soil bulk dielectric permittivity measured by time domain re ectometry: a physical model. Water Resour 35:371–383

Petrik C, Mabee SB (2011) Experimental summarizing the potential of CO_2 sequestration in the basalts of Massachusetts-final report prepared for Massachusetts Clean Energy Center, Boston. http://www.geo.umass.edu/stategeologist/Products/reports/BasaltSequestrationReport.pdf. Accessed 25 July 2018

Plan L (2005) Factors controlling carbonate dissolution rates quantified in a field test in the Austrian alps. Geomorphology 68:201–212

Plug WJ, Moreno LM, Bruining J, Slob EC (2007) Simultaneous measurement of capillary pressure and dielectric constant in porous media. PIERS Online 3(4):549–553

Rabiu KO, Abidoye LK, Das DB (2017) Geo-electrical characterisation for CO_2 sequestration in porous media. Environ Process 4:303. https://doi.org/10.1007/s40710-017-0222-2

Ranganathan P, van Hemert P, Rudolph E, Zitha P (2011) Numerical modelling of CO_2 mineralisation during storage in deep saline aquifers. Energy Procedia 4:4538–4545

Rempel KU, Liebscher A, Heinrich W, Schettler G (2011) An experimental investigation of trace element dissolution in carbon dioxide: applications to the geological storage of CO_2. Chem Geol 289(3–4):224–234

Rust A, Russell J, Knight R (1999) Dielectric constant as a predictor of porosity in dry volcanic rocks. J Volcanol Geotherm Res 91:79–96

Scudiero E, Berti A, Teatini P, Morari F (2012) Simultaneous monitoring of soil water content and salinity with a low-cost capacitance-resistance probe. Sensors (Switz) 12(12):17588–17607. https://doi.org/10.3390/s121217588

Singha K, Li L, Day-Lewis FD, Regberg AB (2012) Quantifying solute transport processes: are chemically "conservative" tracers electrically conservative? Geophysics 76(1):F53–F63

Solomon S, Plattner G-K, Knutti R, Friedlingstein P (2009) Irreversible climate change due to carbon dioxide emissions. Proc Natl Acad Sci USA 106(6):1704–1709

U.S Department of Energy (2008) Shallow carbon sequestration demonstration project. [Online]. http://www.geoengineers.com/sites/default/files/documents/MCSP%20Final%20Report_0-reduced.pdf. Accessed 10 May 2017

Wang L, Mao Z, Shi Y, Tao Q, Cheng Y, Song Y (2014) A novel model of predicting Archie's cementation factor from nuclear magnetic resonance (NMR) logs in low permeability reservoirs. J Earth Sci 25(1):183–188. https://doi.org/10.1007/s12583-014-0411-0

White CM, Strazisar BR, Granite EJ, Hoffman JS, Pennline HW, Air & Waste Management Association (2003) Separation and capture of CO_2 from large stationary sources and sequestration in geological formations-coalbeds and deep saline aquifers. J Air Waste Manag Assoc 53(6):645–715

Wu Z, Yue X, Cheng T, Yu J, Yang H (2014) Effect of viscosity and interfacial tension of surfactant-polymer flooding on oil recovery in high-temperature and high-salinity reservoirs. J Pet Explor Prod Technol 4:9–16. https://doi.org/10.1007/s13202-013-0078-6